Naval Coastal Systems Center

Panama City, Florida 32407-5000

TECHNICAL MEMORANDUM
NCSC TM 492-88

MAY 1990

MODELING TOWED CABLE SYSTEM DYNAMICS

J. W. KAMMAN

T. C. NGUYEN

Approved for public release; distribution is unlimited.

copy

NAVAL COASTAL SYSTEMS CENTER

PANAMA CITY, FLORIDA 32407-5000

CAPT M. W. GAVLAK, USN
Commanding Officer

MR. TED C. BUCKLEY
Technical Director

ADMINISTRATIVE INFORMATION

This report was prepared by the Hydromechanics Branch, Code 2210, of NAVCOASTSYSCEN, in FY 88, in support of the Independent Exploratory Development Program, Subproject Task Area No. ZF55112001, Program No. 62936N, and in support of the NAVCOASTSYSCEN Mine Countermeasures Exploratory Development Project Block Program, Project No. RN15W33, Program Element No. 62315N, from the Office of Naval Technology, 235.

Released by
E. H. Freeman, Head
Advanced Technology
Division

Under authority of
D. P. Skinner, Head
Research and Technology
Department

REPORT DOCUMENTATION PAGE

Form Approved
OMB No. 0704-0188

1. AGENCY USE ONLY ***(Leave blank)***

2. REPORT DATE
APRIL 1990

3. REPORT TYPE AND DATES COVERED

4. TITLE AND SUBTITLE
Modeling Towed Cable System Dynamics

5. FUNDING NUMBERS

6. AUTHOR(S)
J. W. Kamman and T. C. Nguyen

7. PERFORMING ORGANIZATION NAME(S) AND ADDRESS(ES)
Naval Coastal Systems Center
Panama City, Florida 32407-5000

8. PERFORMING ORGANIZATION REPORT NUMBER
NCSC TM 492-88

9. SPONSORING/MONITORING AGENCY NAME(S) AND ADDRESS(ES)

10. SPONSORING/MONITORING AGENCY REPORT NUMBER

11. SUPPLEMENTARY NOTES

12a. DISTRIBUTION/AVAILABILITY STATEMENT
Approved for public release; distribution is unlimited.

12b. DISTRIBUTION CODE

13. ABSTRACT ***(Maximum 200 words)***
A method for modeling the dynamics of towed cable systems is described. The cable system is assumed to be a multiple branched system with towed bodies. These bodies may be spheres or more general vehicles having a single plane of symmetry. The motion of the tow point of the system is arbitrary. The cable is modeled by a series of rigid cylinders connected end-to-end by spherical joints. It is further assumed that the physical parameters of the system and the external forces acting on it can be lumped at the connecting joints. The towed vehicles are three-dimensional bodies with linear (about a steady-state configuration) time-domain analyses. Examples are used to illustrate the analyses.

14. SUBJECT TERMS
Hydromechanics; Cable Dynamics; Towed Cables; Submerged Cables; Modeling; CABLE3D Computer Program.

15. NUMBER OF PAGES
26

16. PRICE CODE

17. SECURITY CLASSIFICATION OF REPORT	18. SECURITY CLASSIFICATION OF THIS PAGE	19. SECURITY CLASSIFICATION OF ABSTRACT	20. LIMITATION OF ABSTRACT
UNCLASSIFIED	UNCLASSIFIED	UNCLASSIFIED	SAR

NSN 7540-01-280-5500

Standard Form 298 (Rev. 2-89)
Prescribed by ANSI Std. Z39-18
298-102

CONTENTS

ILLUSTRATIONS

INTRODUCTION

Modeling of submerged cable dynamics has been of interest for at least the past 30 years. References 1 through 11 represent a partial list of the many works on this subject covering continuum, finite element, finite segment, and lumped parameter approaches. Reference 12 provides an excellent survey of the work done prior to 1973.

In a series of recent papers,[6,13-15] a method was presented based on previously developed general procedures for finite segment modeling of multibody systems.[16,17] In that work cables were modeled by a series of rigid cylinders connected end-to-end by ball-and-socket joints. In particular, in references 14 and 15 the model was partially validated by comparing model predictions with predictions of linear partial differential equation models[18,19] developed from continuum assumptions and with experimental data recorded at the Civil Engineering Laboratory at Port Hueneme, California.[20] As a result of this work, computer programs were developed[21-23] for the three-dimensional simulation of submerged and partially submerged cable dynamics.

The computer program CABLE3D[23] developed at the Naval Coastal Systems Center (NAVCOASTSYSCEN) has been applied to many towed cable systems. However, its utility is limited by extremely long execution times that make the program expensive to use. In 1987 NAVCOASTSYSCEN contracted with the University of Alabama to investigate speed improvements to the CABLE3D code to make it a more viable modeling tool. The results of this investigation are documented in their report.[24]

For many submerged towed cable systems, the viscous forces acting on the cable are large compared to the weight forces. Using a lumped parameter model and an analytical approach similar to that in reference 1, it is shown in reference 24 that for these systems (and possibly others where viscous forces do not dominate) a lumped parameter model is sufficient to model the system dynamics. Furthermore, it is shown that a substantial increase in execution speed can be achieved (over the computer programs described in references 21 through 23) using this method. With this motivation, the equations of motion are developed herein using an approach similar to that in references 1 and 24. The lumped parameter model is described in the following paragraphs.

A towed cable system is assumed to be a multiple branched cable system with towed bodies. The system is assumed to be pulled from a single tow point (Figure 1). The cable and its branches form an open tree system having no closed kinematic chains. Each length of cable may have different physical properties, and the towed bodies may be spheres or more general vehicles with a single plane of symmetry. The motion of the system tow point is arbitrary.

The system is modeled using discrete elements. This allows straightforward formulation of the equations of motion for systems with branches and allows physical parameters to be changed from element to element. Moreover, the use of simple elements simplifies the solution process.

The cable is modeled by a series of rigid links connected by frictionless spherical joints. The masses of the links are concentrated half at each of their ends, the connecting joints of the system. All fluid drag, added mass, weight, and buoyancy forces are also concentrated at the connecting joints. Hence, the cable links are two-force members, carrying forces only along their length. The links are also assumed to be small enough so that the forces acting on them are approximately uniform over their length.

The spherical towed bodies are assumed to be concentrated masses coincident with the lumped mass of the connecting cable link. The nonspherical towed vehicles are three-dimensional bodies with mass and inertia. They are connected to their adjacent cable links by frictionless spherical joints at some reference point in the vehicle. This reference point need not be located at the vehicle's mass center.

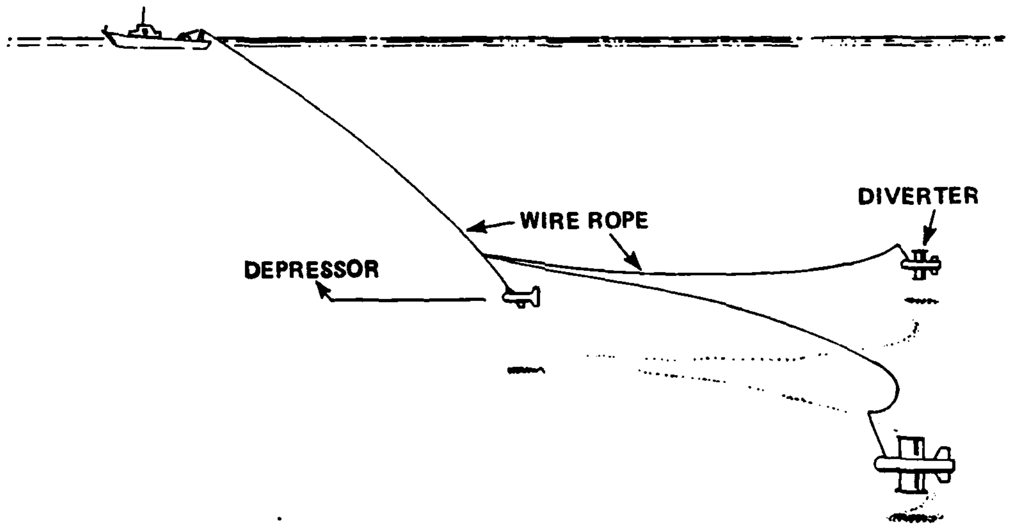

FIGURE 1. TOWED CABLE SYSTEM

The remainder of this report is divided into five parts. The first three parts give details on the equations required to describe the system kinematics and dynamics. The fourth describes a set of numerical examples that illustrate the capabilities of the analysis. Results and execution times required by the analysis presented in this paper are compared with those required by the computer program CABLE3D[23] in the last of the examples. The final section contains a short discussion.

KINEMATICS

SYSTEM CONFIGURATION

The position of the system tow point is described by specifying the position and orientation of the mean ship frame together with the motion of the tow point relative to the mean ship frame. The ship frame indicates the forward (X_m), starboard (Y_m), and downward (Z_m) directions. It provides a convenient reference frame for describing the configuration of the system, especially during steady-state motions.

At time t = 0, the X_m (forward), Y_m (starboard), and Z_m (downward) axes of the mean ship frame are assumed to be coincident with the X_i, Y_i, and Z_i axes of the inertial reference frame. As time progresses the ship frame is assumed to move in a horizontal plane relative to the inertial frame. Its position is given by the X_i and Y_i coordinates of its origin and its orientation is given by a single

turning angle ψ measured as positive when the ship is in a starboard turn. The orientation of the mean ship frame (M) can be related to the orientation of the inertial reference frame (R) through the following transformation matrix:

$$S(R,M) = \begin{bmatrix} C_\psi & -S_\psi & 0 \\ S_\psi & C_\psi & 0 \\ 0 & 0 & 1 \end{bmatrix} \tag{1}$$

The configuration of the rest of the towed cable system at any instant of time is described by a sequence of orientation angles measured relative to the mean ship frame. The orientation of each cable link is given by two angles and the orientation of each towed vehicle is given by three angles. Since the mass and external forces acting on a towed sphere are lumped with the mass at the end of its connecting cable link, no additional angles are needed for them. Hence, for a model with a total of NC cable links and NT towed bodies, there are 2NC + 3NT total angles needed to define the configuration of the system. This is also the number of degrees-of-freedom of the model.

The orientation of the cable links is described by a dextral 2-3 rotation sequence. First, align the cable link along the $-X_m$ axis and affix a set of axes x, y, and z to the link parallel to the ship frame axes X_m, Y_m, and Z_m, respectively. Then rotate the link downward about the y (Y_m) axis through an angle θ_1, and then outward about the z axis (which is perpendicular to the link) through an angle θ_2 (Figure 2). The X', Y', and Z' axes represent the directions of the x, y, and z axes, respectively, after the first rotation. Note that since the masses of the links are to be lumped at the connecting joints, the moment of inertia of the links are ignored, making a third orientation angle superfluous.

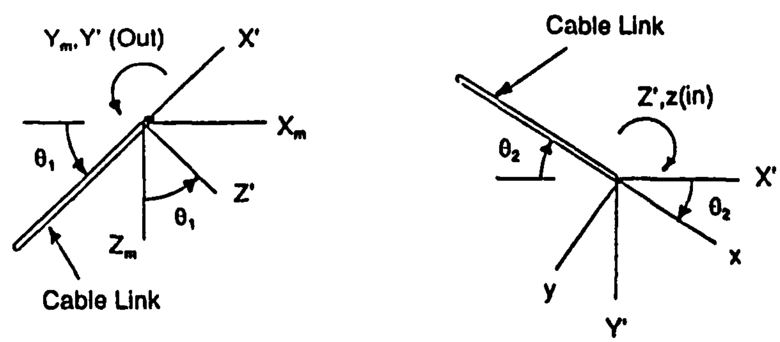

FIGURE 2. ORIENTATION ANGLES FOR CABLE LINKS

The orientation of the towed vehicles are given by a dextral 1-2-3 rotation sequence relative to the mean ship frame. That is, the dextral rotations θ_1, θ_2, and θ_3 occur about the vehicle-fixed x, y, and z axes, respectively. The x, y, and z axes are assumed to represent the axial (roll), lateral (pitch), and normal (yaw) directions of the towed vehicle.[25] As for the cable links, these axes are parallel to the ship frame axes when the values of the orientation angles are zero (Figure 3). For this rotation sequence, the orientation of the vehicle-fixed frame (K) can be related to that of the mean ship frame (M) through the following transformation matrix:

$$S(M,K) = \begin{bmatrix} C_2 C_3 & -C_2 S_3 & S_2 \\ S_1 S_2 C_3 + S_3 C_1 & -S_1 S_2 S_3 + C_3 C_1 & -S_1 C_2 \\ -C_1 S_2 C_3 + S_3 S_1 & C_1 S_2 S_3 + C_3 S_1 & C_1 C_2 \end{bmatrix} \qquad (2)$$

It should be noted here that the orientation of the vehicle can be related to the inertial frame by multiplying the transformation matrices of equations (1) and (2). That is,

$$S(R,K) = S(R,M)\, S(M,K) \qquad (3)$$

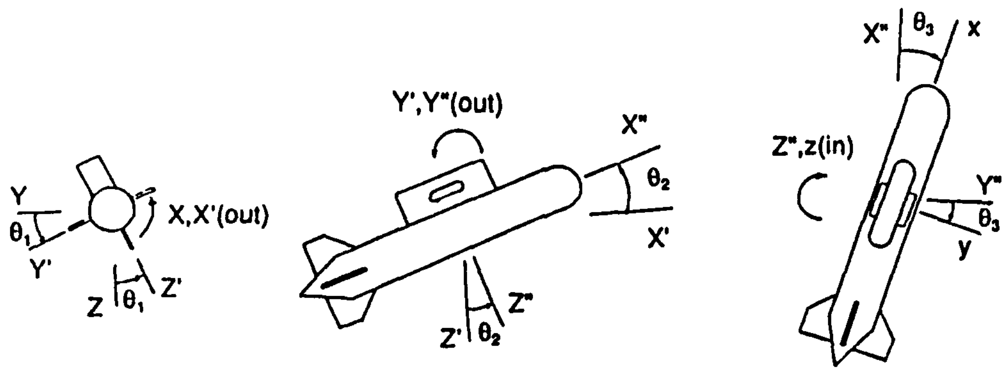

FIGURE 3. ORIENTATION ANGLES FOR TOWED VEHICLES

SYSTEM MOTION

Given the motion of the mean ship frame, the motion of the system tow point relative to this frame, the orientation angles described above, and the time derivatives of the orientation angles, then the motion of the system model may be determined. The following paragraphs outline this process.

Consider a typical cable link L_K with ends J and K. Here J is assumed to be located at the upper end of the link, closer to the system tow point. The position vector $\mathbf{P}^K$ of end K relative to an inertial reference frame may be written in terms of $\mathbf{P}^J$ the position vector of end J as follows:

$$\mathbf{P}^K = \mathbf{P}^J + \mathbf{p}^K \qquad (4)$$

where

$$\mathbf{p}^K = L^K \mathbf{n}^K \qquad (5)$$

$$\mathbf{n}^K = -C_1^K C_2^K \mathbf{m}_1 - S_2^K \mathbf{m}_2 - S_1^K C_2^K \mathbf{m}_3 \qquad (6)$$

where the S^K and C^K represent the sin (θ^K) and the cos (θ^K), respectively, and the $\mathbf{m}_i$ (i = 1, 2, 3) represent unit vectors fixed in the mean ship frame. Note here that using equation (4) and $\mathbf{P}^0$ the position vector of the system tow point, the position vectors of the end points of all the cable links can be determined.

Equation (4) may now be differentiated to give the velocities and accelerations of the ends of the links as follows:

$$\mathbf{V}^K = \mathbf{V}^J + \dot{\mathbf{p}}^K \tag{7}$$

$$\mathbf{A}^K = \mathbf{A}^J + \ddot{\mathbf{p}}^K \tag{8}$$

where

$$\dot{\mathbf{p}}^K = \mathbf{p}_i^K \; \dot{\theta}_i^K + \mathbf{p}_\psi^K \; \dot{\psi} \tag{9}$$

$$\ddot{\mathbf{p}}^K = \mathbf{p}_i^K \; \ddot{\theta}_i^K + \dot{\mathbf{p}}_i^K \; \dot{\theta}_i^K + \mathbf{p}_\psi^K \; \ddot{\psi} + \dot{\mathbf{p}}_\psi^K \; \dot{\psi} \tag{10}$$

and where $\mathbf{p}_i^K$ and $\mathbf{p}_\psi^K$ represent the partial derivatives of $\mathbf{p}^K$ with respect to θ_i^K (i = 1, 2) and ψ, respectively, and the dots represent time differentiation. Explicit forms for $\dot{\mathbf{p}}^K$ and $\ddot{\mathbf{p}}^K$ may be found by performing the necessary differentiations of $\mathbf{p}^K$ as given by equations (5) and (6). In the numerical procedure presented in the sequel explicit forms are required only for $\dot{\mathbf{p}}^K$. Regarding notation, repeated subscripts (such as i in the above equations) represent a sum over the range of that index. This notation will be used consistently throughout the remainder of this paper.

The above equations provide components of the positions, velocities, and accelerations of the lumped masses as a function of the ship motion, the cable link angles, and the link angle derivatives. Later in this analysis, it will be necessary to calculate the second derivatives of the link angles from the acceleration components. To this end, noting that $\mathbf{p}_1^K \cdot \mathbf{p}_2^K$ is zero, it was shown in reference 24 that:

$$\ddot{\theta}_i^K = \frac{[\mathbf{A}^K - \mathbf{A}^J - \dot{\mathbf{p}}_j^K \, \dot{\theta}_j^K - \mathbf{p}_\psi^K \, \ddot{\psi} - \dot{\mathbf{p}}_\psi^K \, \dot{\psi}] \cdot \mathbf{p}_i^K}{\mathbf{p}_i^K \cdot \mathbf{p}_i^K} \tag{11}$$

for i = 1, 2. Hence, given the lumped mass accelerations components, the link angles, and the link angle derivatives, the second derivatives of the link angles can be calculated. Note here again that there is a sum in equation (11) over the range of the repeated index j from 1 to 2.

Consider next a typical towed vehicle. Given the orientation angles and their time derivatives (1-2-3 rotation sequence as presented earlier) for the towed vehicle, the angular velocity and angular acceleration of the vehicle may be written as follows:[26]

$$\mathbf{w} = \omega_i \, \mathbf{b}_i \quad \text{and} \quad \dot{\mathbf{w}} = \dot{\omega}_i \, \mathbf{b}_i \tag{12}$$

where the $\mathbf{b}_i$ are unit vectors fixed in the vehicle and

$$\omega_1 = C_2 C_3 \dot{\theta}_1^K + S_3 \dot{\theta}_2^K + \dot{\psi}(S_1 S_3 - C_1 S_2 C_3) \tag{13}$$

$$\omega_2 = -C_2 S_3 \dot{\theta}_1^K + C_3 \dot{\theta}_2^K + \dot{\psi}(S_1 C_3 + C_1 S_2 S_3) \tag{14}$$

$$\omega_3 = S_2 \dot{\theta}_1^K + \dot{\theta}_3^K + C_1 C_2 \dot{\psi} \tag{15}$$

The velocity of the mass center of the vehicle can then be determined as follows:

$$\mathbf{V}^K = \mathbf{V}^J + \mathbf{w}\, x\, \mathbf{p}^K \tag{16}$$

where $\mathbf{V}^J$ represents the velocity of J the lumped mass at the end of the adjacent cable link and $\mathbf{p}^K$ represents the position vector of the mass center of the vehicle relative to J.

Equations (13) through (15) may also be inverted to give[26]

$$\dot{\theta}_1^K = C_3[\omega_1 - \dot{\psi}(S_1 S_3 - C_1 S_2 C_3)] / C_2 - S_3[\omega_2 - \dot{\psi}(S_1 C_3 + C_1 S_2 S_3)] / C_2 \tag{17}$$

$$\dot{\theta}_2^K = S_3[\omega_1 - \dot{\psi}(S_1 S_3 - C_1 S_2 C_3)] + C_3[\omega_2 - \dot{\psi}(S_1 C_3 + C_1 S_2 S_3)] \tag{18}$$

$$\begin{aligned}\dot{\theta}_3^K = {} & \omega_3 - \dot{\psi} C_1 C_2 - S_2 C_3[\omega_1 - \dot{\psi}(S_1 S_3 - C_1 S_2 C_3)] / C_2 \\ & + S_2 S_3[\omega_2 - \dot{\psi}(S_1 C_3 + C_1 S_2 S_3)] / C_2\end{aligned} \tag{19}$$

These equations may now be differentiated to give explicit equations for calculating the second derivatives of a vehicle's orientation angles given the components of its angular acceleration vector (along the vehicle-fixed directions), the orientation angles and their first derivatives, and the angular motion of the mean ship frame.

NONLINEAR EQUATIONS OF MOTION

EQUATIONS OF MOTION

The equations of motion of the system model can be found by applying Newton's law of motion to each of the model's components. In general, these equations may be written as follows:

$$M_{ij}^K \ddot{y}_j^K = f_i^K \quad \text{or} \quad \ddot{y}_i^K = \hat{M}_{ij}^K f_j^K \tag{20}$$

where the $\ddot{y}_i^K$ represents $\ddot{x}_i^K$ (i = 1, 2, 3) the inertial acceleration components of the lumped masses and $\ddot{x}_i^K$ (i = 1, 2, 3) and $\dot{\omega}_i^K$ (i = 1, 2, 3) the mass center acceleration components and angular acceleration components of the towed vehicles in the vehicle-fixed frame. The range of the subscripts i and j in equation (20) are thus from 1 to 3 for lumped masses and from 1 to 6 for towed vehicles, and the definitions of M_{ij}^K and f_i^K depend, of course, on the particular model component. Note here also that $\hat{M}_{ij}^K$ in equation (20) represents the inverse of matrix M_{ij}^K.

For the general lumped mass shown in Figure 4 we have

$$M_{ij}^{K} = \left(m^{L} + m^{K} + A^{L} + A^{K} + \sum_{H} A^{H}\right)\delta_{ij} - A^{K} n_i^{K} n_j^{K} - \sum_{H} A^{H} n_i^{H} n_j^{H} \quad (i,j = 1,2,3) \tag{21}$$

$$f_i^{K} = -t^{K} n_i^{K} + \sum_{H} t^{H} n_i^{H} + (\mathbf{Q}^{K} + \mathbf{Q}^{L}) \cdot \mathbf{i}_i \quad (i = 1,2,3) \tag{22}$$

where $\mathbf{i}_i$ represent unit vectors fixed in an inertial reference frame and δ_{ij} represents the standard Kronecker delta symbol.[27] The entries in the symmetric mass matrix M_{ij}^{K} include m^L the mass of the sphere, m^K half the total mass of all the adjacent cable links, A^L the added mass of the sphere, A^K and A^H, ($H = K_1, \ldots, K_m$) half the added masses of the adjacent cable links, and n_i^J ($J = K, K_1, \ldots, K_m$) the inertial components of the unit vectors $\mathbf{n}^J$ (which are parallel to the links). The values of the added mass entries are taken to be:

$$A^{L} = \frac{1}{2}\, C_M\, \rho V^{L} \tag{23}$$

$$A^{J} = \frac{1}{2}\, C_M\, \rho V^{J} \tag{24}$$

where C_M is the added mass coefficient, ρ is the density of the fluid, and V^L and V^J ($J = K, K_1, \ldots, K_m$) denote the volumes of the sphere and the adjacent cable links, respectively. Note that A^L and A^J are defined as in references 5 and 13 except for the link added masses that are multiplied by a factor of one-half for distribution to the lumped masses. The vector f_i^K includes t^J the internal cable tensions, Q^L the resultant of the drag, buoyancy, and weight forces acting on the sphere, and Q^K half the resultant of the drag, buoyancy, and weight forces acting on all adjacent cable links. Note that these forces are also taken as presented in references 5 and 13, with drag forces assumed constant over the cable links. As with the mass and added mass distributions, the forces on the cable links are all distributed half at each end.

Consider next a lumped mass attached to a towed vehicle in Figure 5. In this case the entries M_{ij}^K and f_i^K become:

$$M_{ij}^{K} = (m^{K} + A^{K})\,\delta_{ij} - A^{K} n_i^{K} n_j^{K} \qquad (i,j = 1,2,3) \tag{25}$$

$$f_i^{K} = -t^{K} n_i^{K} + S(R,L)_{ij}\, t_j^{L} + (\mathbf{Q}^{K}) \cdot \mathbf{i}_i \qquad (i = 1,2,3) \tag{26}$$

where, as before, m^K represents half the mass and A^K represents half the added mass on the adjacent cable link K, n_i^K represents the inertial components of a unit vector parallel to the link K, t^K represents the force in link K, Q^K represents half the resultant of the fluid drag, buoyancy, and weight forces on link K, and t_j^L represents the components of the force acting on the lumped mass due to the adjacent towed body along vehicle-fixed directions. The matrix S(R,L) is the transformation matrix relating the orientation of towed vehicle L to the inertial reference frame.

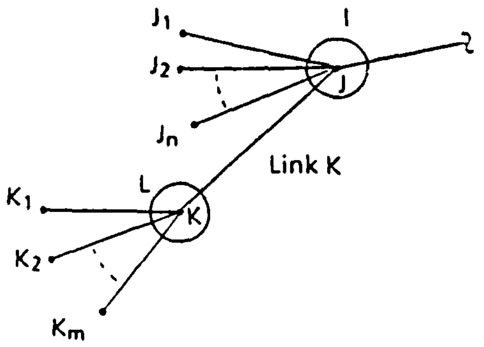

FIGURE 4. GENERAL LUMPED MASS

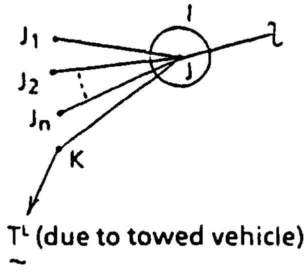

FIGURE 5. LUMPED MASS ATTACHED TO A TOWED VEHICLE

Finally, consider a typical towed vehicle as shown in Figure 6. The force $-\mathbf{T}^K$ is the three component force located at cable attachment point. The unit vectors $\mathbf{b}_i$ are fixed in the body and indicate the axial, lateral, and normal body directions as presented in reference 25. At any instant, the velocity of the mass center K relative to the surrounding fluid and the angular velocity of the body may be written as follows:

$$\mathbf{V}^{K/W} = u_i^K \mathbf{b}_i \quad \text{and} \quad \mathbf{w}^K = \omega_i^K \mathbf{b}_i \quad . \tag{27}$$

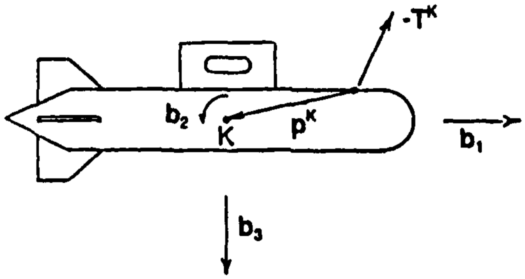

FIGURE 6. TOWED VEHICLE AND ATTACH POINT

The fluid drag force acting on the vehicle is assumed to be given as a function of the u_i^K, the ω_i^K, and a set of hydrodynamic coefficients similar to those in reference 25. The added mass force and moment acting on the vehicle are assumed to be given as follows:

$$\mathbf{F}_M^K = X_{ij}^K \dot{v}_j^K \mathbf{b}_i \quad (i = 1,2,3; \quad j = 1, \ldots, 6) \tag{28}$$

$$\mathbf{M}_M^K = N_{ij}^K \dot{v}_i^K \mathbf{b}_i \quad (i = 1,2,3; \quad j = 1, \ldots, 6) \tag{29}$$

where

$$v_i^K = u_i^K \quad (i = 1,2,3) \tag{30}$$

$$v_i^K = \omega_{i-3}^K \quad (i = 4,5,6) \tag{31}$$

and the X_{ij}^K and N_{ij}^K are a specified set of coefficients again similar to those in reference 25.

Using this notation, M_{ij}^K and f_i^K of equation (20) for a towed vehicle may be written as follows:

$$M_{ij}^K = m^K \delta_{ij} - X_{ij}^K \quad (i,j = 1,2,3) \tag{32}$$

$$M_{ij}^K = -X_{ij}^K \quad (i = 1,2,3; \quad j = 4,5,6) \tag{33}$$

$$M_{ij}^K = -N_{i-3,j}^K \quad (i = 4,5,6; \quad j = 1,2,3) \tag{34}$$

$$M_{ij}^K = I_{i-3,j-3}^K \; - N_{i-3,j}^K \quad (i,j = 4,5,6) \tag{35}$$

$$f_i^K = (\mathbf{Q}^K - \mathbf{T}^K) \cdot \mathbf{b}_i - (\mathbf{w}^K \, x \, \mathbf{V}^K) \cdot (X_{ij}^K \, \mathbf{b}_j) \quad (i,j = 1,2,3) \tag{36}$$

$$f_l^K = (\mathbf{M}_T^K + \mathbf{M}_Q^K - \mathbf{w}^K \, x \, \mathbf{I}^K \cdot \mathbf{w}^K) \cdot \mathbf{b}_{i-3} \quad - (\mathbf{w}^K \, x \, \mathbf{V}^K) \cdot (N_{i-3,j}^K \, \mathbf{b}_j)$$
$$(j = 1,2,3; \quad i = 4,5,6) \tag{37}$$

where $\mathbf{I}^K$ is the inertia tensor of the vehicle about a set of axes through the mass center of the body and parallel to the unit vectors $\mathbf{b}_i$, $\mathbf{V}^K$ is the velocity of the mass center of the vehicle, $\mathbf{Q}^K$ is the resultant of the fluid drag, buoyancy, and weight forces acting on the vehicle, $\mathbf{M}_T^K$ and $\mathbf{M}_Q^K$ are the moments of -$\mathbf{T}^K$ and $\mathbf{Q}^K$ about the mass center of the vehicle, respectively.

INTERNAL CABLE FORCES

In order to calculate the internal cable forces at any time, a set of additional equations must be introduced to impose the condition of rigidity on the cable links and towed vehicles. These equations of constraint relate the Cartesian coordinates, velocities, and accelerations of adjacent lumped masses and adjacent lumped masses and vehicle mass centers. In particular, for a cable link (two adjacent lumped masses) we have

$$\mathbf{p}^K \cdot \mathbf{p}^K = (L^K)^2 \quad . \tag{38}$$

Differentiating this equation twice with respect to time gives

$$(\ddot{x}_i^K - \ddot{x}_i^J)\, L^K n_i^K \;=\; -\dot{\mathbf{p}}^K \cdot \dot{\mathbf{p}}^K \tag{39}$$

Here J and K refer to the lumped masses at the ends of link K as shown in Figure 4. For a towed vehicle (adjacent lumped mass and towed vehicle mass center) the equation of constraint is

$$\mathbf{A}^{K/J} \;=\; \mathbf{A}^K - \mathbf{A}^J = \dot{\mathbf{w}}^K x\, \mathbf{p}^K + \mathbf{w}^K x\, \dot{\mathbf{p}}^K \quad . \tag{40}$$

In vehicle-fixed component form this equation becomes

$$S(R,K)_{ji}\, \ddot{x}_j^J \;-\; \ddot{x}_i^K \;+\; P_{im}^K\, \dot{\omega}_m^K \;=\; -[\mathbf{w}^K x\, (\mathbf{w}^K x\, \mathbf{p}^K)] \cdot \mathbf{b}_i \tag{41}$$

where $\ddot{x}_i^J$ (i = 1, 2, 3) represent the inertial components of the acceleration of lumped mass J, $\ddot{x}_i^K$ (i = 1, 2, 3) and $\dot{\omega}_i^K$ (i = 1, 2, 3) represent the components of the acceleration of the mass center and the angular acceleration of the vehicle about the vehicle-fixed axes, and P_{im}^K (i,m = 1, 2, 3) are defined as follows:

$$P_{im}^K \;=\; e_{kim}\, p_k^K \tag{42}$$

where e_{kim} is the permutation symbol,[27] and p_k^K represents the vehicle-fixed components of $\mathbf{p}^K$ the vector from the cable attachment point to the mass center of the body as shown in Figure 6.

Substituting from equations (20), (22), (26), (36), and (37) into equations (39) and (41) results in a set of equations that are linear in the internal cable forces and force components (in the case of a towed vehicle).

In the following paragraphs the results for general lumped masses, lumped masses attached to towed vehicles, and towed vehicles are presented. Note that the results are given for the cases with and without added mass effects. Note that the effect of added mass complicates the equations considerably, especially for the cable links. (See the Numerical Solution section below for further comments.)

For the general lumped mass shown in Figure 4 we have

$$\begin{aligned}
&[\hat{M}_{ij}^J\, n_i^K\, n_j^J]\, t^J \;-\; \sum_G [\hat{M}_{ij}^J\, n_i^K\, n_j^G]\, t^G \;-\; [(\hat{M}_{ij}^K + \hat{M}_{ij}^J)\, n_i^K\, n_j^K]\, t^K \\
&+ \sum_H [\hat{M}_{ij}^K\, n_i^K\, n_j^H]\, t^H \;=\; -L^K (\dot{n}^K)^2 \;+\; n_i^K\, [\hat{M}_{ij}^J\, (Q_j^I + Q_j^J) - \hat{M}_{ij}^K\, (Q_j^L + Q_j^K)]
\end{aligned} \tag{43}$$

where there is a sum over the repeated indices i and j from 1 to 3, the sum over G ranges from J_1 to J_n, the sum over H ranges from K_1 to K_m, and Q_j^M (M = I, J, K, and L) represents the inertial components of $\mathbf{Q}^M$ the external force vectors. All other symbols are as previously defined. If the added mass effect is neglected this equation reduces to

$$[\mu^J n_i^K n_i^J]\, t^J \;-\; \sum_G [\mu^J n_i^K n_i^G]\, t^G \;-\; [\mu^K + \mu^J]\, t^K$$

$$+\sum_H [\mu^K n_i^K n_i^H]\, t^H \;=\; -L^K (\dot{n}^K)^2 \;+\; n_i^K [\mu^J (Q_i^I + Q_i^J) \;-\; \mu^K (Q_i^L + Q_i^K)] \quad . \qquad (44)$$

where μ^K represents the inverted sum of the masses associated with lumped mass K.

In the case of a lumped mass attached to the towed vehicle, the resulting equation is

$$[\hat{M}_{ij}^J n_i^K n_j^J]\, t^J \;-\; \sum_G [\hat{M}_{ij}^J n_i^K n_j^G]\, t^G \;-\; [(\hat{M}_{ij}^K + \hat{M}_{ij}^J)\, n_i^K n_j^K]\, t^K$$

$$+[\hat{M}_{ij}^K n_i^K S(R,L)_{jk}]\, t_k^L \;=\; -L^K (\dot{n}^K)^2 \;+\; n_i^K [\hat{M}_{ij}^J (Q_j^I + Q_j^J) \;-\; \hat{M}_{ij}^K Q_j^K] \quad . \qquad (45)$$

When the added mass effect is neglected, this equation reduces to

$$[\mu^J n_i^K n_i^J]\, t^J \;-\; \sum_G [\mu^J n_i^K n_i^G]\, t^G \;-\; [\mu^K + \mu^J]\, t^K$$

$$+[\mu^K n_i^K S(R,L)_{ik}]\, t_k^L \;=\; -L^K (\dot{n}^K)^2 \;+\; n_i^K [\mu^J (Q_i^I + Q_i^J) \;-\; \mu^K Q_i^K] \quad . \qquad (46)$$

Finally, for the case of a towed vehicle we have

$$-S(R,K)_{ji} \;\; \hat{M}_{jk}^J n_k^J t^J \;+\; D_{in}^K t_n^K \;=\; \mathbf{d}^K \cdot \mathbf{b}_i \;-\; S(R,K)_{mi} \hat{M}_{mk}^J Q_k^J$$

$$+[\hat{M}_{ij}^K - P_{ik}^K \hat{M}_{k+3,j}^K]\, \{Q_j^K \;-\; \mathbf{e}^K \cdot (X_{jm}^K \mathbf{b}_m)\}$$

$$+[\hat{M}_{i,j+3}^K - P_{ik}^K \hat{M}_{k+3,j+3}^K]\, \{M_{Qj}^K - \mathbf{g}^K \cdot \mathbf{b}_j - \mathbf{e}^K \cdot (N_{jm}^K \mathbf{b}_m)\} \quad (i = 1,2,3) \qquad (47)$$

where

$$D_{in}^K \;=\; S(R,K)_{ji} \hat{M}_{jk}^J S(R,K)_{kn} \;+\; \hat{M}_{in}^K \;+\; \hat{M}_{i,j+3}^K P_{jn}^K \;-\; P_{ik}^K \hat{M}_{k+3,n}^K$$

$$-P_{ik}^K \hat{M}_{k+3,j+3}^K P_{jn}^K \quad (i, n = 1,2,3) \qquad (48)$$

$$\mathbf{d}^K \;=\; -[\mathbf{w}^K x\, (\mathbf{w}^K x\, \boldsymbol{\rho}^K)] \qquad (49)$$

$$\mathbf{g}^K \;=\; \mathbf{w}^K x\, \mathbf{I}^K \cdot \mathbf{w}^K \qquad (50)$$

$$\mathbf{e}^K \;=\; \mathbf{w}^K x\, \mathbf{V}^K \qquad (51)$$

where Q_j^k and M_{Qj}^K are the components of the vectors $\mathbf{Q}^K$ and $\mathbf{M}_Q^K$ along the vehicle-fixed directions, and Q_k^J are the inertial components of vector $\mathbf{Q}^J$. When the added mass effect is neglected, the above equation reduces to

$$[-\mu^J S(R,K)_{ji}\, n_j^J]\, t^J \quad + \quad [\mu^K + \mu^J]\, t_i^K \quad - \quad [P_{ik}^k\, I_{kj}^K\, P_{jn}^K]\, t_n^K$$

$$= \mathbf{d}^K \cdot \mathbf{b}_i \quad + \quad (\mu^K\, Q_i^K - \mu^J\, Q_i^J) \quad + \quad P_{ik}^K\, I_{kj}^K\, (g_j^K - M_{Qj}^K) \quad (i = 1,2,3) \tag{52}$$

where Q_i^K, Q_i^J, M_{Qj}^K, and g_j^K are the components of vectors $\mathbf{Q}^K, \mathbf{Q}^J, \mathbf{M}_Q^K$, and $\mathbf{g}^K$ about the vehicle-fixed directions, and I_{kj}^K are the vehicle-fixed components of the inverse of the vehicle's inertia matrix.

NUMERICAL SOLUTION

Given the model's physical data, the motion of the mean ship frame, the motion of the system tow point relative to the mean ship frame, the initial orientation angles of the system and their first derivatives at some initial time t_o, the following procedure is used to determine the motion of the cable system model at a sequence of later times. First, determine the components of position and velocity vectors of the lumped masses, the position and velocity vectors of the mass centers, and the angular velocity vectors of the towed vehicles. Then determine the external forces acting on the system. Then, using these results and equations (43) through (52), formulate and solve a set of linear equations for the internal cable forces. Then use equation (20) along with the cable forces to calculate the accelerations of the lumped masses and the accelerations of the mass centers and the angular accelerations of the towed vehicles. Finally, use equations (11) and (17) through (19) ((17) through (19) must be differentiated with respect to time) to determine the second time derivatives of the orientation angles. These values can be used in a numerical integration scheme to find the orientation angles and their first time derivatives at the next time step. The procedure may be repeated to determine the motion of the system at later times.

When the added mass effect is included, the equations of motion become more complex. Including the effect for cable links produces 3x3 mass matrices M_{ij}^K that are time dependent and, hence, must be calculated and inverted at each time step. This is a heavy numerical burden. This time-dependency results from assuming that the added mass effects are present only when the cable is accelerating (relative to the fluid) normal to its length. The problems are not as severe for towed vehicles or spheres. In these cases, the mass matrices are not time dependent.

LINEAR EQUATIONS OF MOTION

In general, the nonlinear equations of motion for the towed cable system model may be expressed in the form:

$$\dot{y}_i \;=\; f_i(y_j) \;=\; y_{n+i} \quad (i = 1,\ldots,n;\;\; j = 1,\ldots,2n) \tag{53}$$

$$\dot{y}_i \;=\; f_i(y_j, u_k) \quad (i = n+1,\ldots,2n;\;\; j = 1,\ldots,2n;\;\; k = 1,\ldots,m) \tag{54}$$

where y_i (i = 1, . . . , n) represent the orientation angles relative to the mean ship frame of the cable links and towed vehicles of the system. y_i (i = n + 1, . . . , 2n) represent the first derivatives of these angles, and u_k (k = 1, . . . , m) represent a set of external inputs, such as tow point motion and control surface motions on the towed vehicles. During steady forward or steady turning motion and in the absence of external disturbances, the system can exhibit steady-state equilibrium positions. In these situations, the orientation angles relative to the mean ship frame remain constant. These angles may be found by solving the n nonlinear algebraic equations

$$f_{n+i}\,(y_{je}\,,\,y_{n+j,e} = 0) \;=\; 0 \quad (i,j = 1,\ldots,n) \tag{55}$$

where y_{je} and $y_{n+j,e}$ (j = 1, . . . , n) represent the equilibrium values of the orientation angles of the system and their time derivatives, respectively.

To describe motions of the system that result from small disturbances to the state vector **y** or to the external input vector **u**, the nonlinear equations of motion ((53) and (54)) can be linearized about the equilibrium configuration. To this end, introduce a perturbation vector **z** to the equilibrium state vector $\mathbf{y}_e$ and a perturbation vector **v** to the equilibrium external input vector $\mathbf{u}_e$ so that

$$y_i \;=\; y_{ie} \;+\; z_i \quad (i = 1,\ldots,2n) \tag{56}$$

$$u_k \;=\; u_{ke} \;+\; v_k \quad (k = 1,\ldots,m)\;\;. \tag{57}$$

Substituting these values into the nonlinear equations of motion, expanding in a Taylor Series about the equilibrium configuration, and omitting terms of second for higher order in the perturbations z_i and v_k results in the equations

$$\dot{z}_i \;=\; A_{ij}\,z_j \;+\; B_{ik}\,v_k \tag{58}$$

where

$$A_{ij} \;=\; (\partial f_i \,/\, \partial y_j\,)_e \tag{59}$$

$$B_{ik} \;=\; (\partial f_i \,/\, \partial u_k\,)_e \quad . \tag{60}$$

Here the subscript e on the partial derivatives indicates that they are evaluated at the equilibrium configuration. Since the first n equations (53) are simply definitions of the state vector **y**, the first n rows of the **A** and **B** matrices take on the special values

$$A_{ij} \;=\; 0 \quad (i,j = 1,\ldots,n) \tag{61}$$

$$A_{i,n+j} \;=\; \delta_{ij} \quad (i,j = 1,\ldots,n) \tag{62}$$

$$B_{ik} \;=\; 0 \quad (i = 1,\ldots,n;\quad k = 1,\ldots,m) \tag{63}$$

where, as before, δ_{ij} represents the standard Kronecker delta symbol.

The nontrivial entries in the matrices may be approximated using finite differences. In this work a second-order central difference is used so that the entries are calculated as follows:

$$A_{ij} = \frac{f_i(\mathbf{y}_e + \mathbf{dy}_j, \mathbf{u}_e) - f_i(\mathbf{y}_e - \mathbf{dy}_j, \mathbf{u}_e)}{2dy_j} \tag{64}$$

$$B_{ik} = \frac{f_i(\mathbf{y}_e, \mathbf{u}_e + \mathbf{du}_k) - f_i(\mathbf{y}_e, \mathbf{u}_e - \mathbf{du}_k)}{2du_k} \tag{65}$$

where dy_j and du_k represent small increments in y_j, and u_k; $\mathbf{dy}_j$ represents the 2n-vector of increments $(0, \ldots, 0, dy_j, 0 \ldots, 0)$ and $\mathbf{du}_k$ represents the m-vector of increments $(0, \ldots, 0, du_k, 0, \ldots, 0)$. The nonzero increments dy_j and du_k occur in the j^{th} and k^{th} entries of $\mathbf{dy}_j$ and $\mathbf{du}_k$, respectively. Note that since the steady-state motion is stationary, the matrices **A** and **B** are constant matrices.

Equation (58) represents a set of first-order linear system of equations in the perturbations **z** and **v**. They are useful for studying towed system stability, sensitivity to change of input state **v**, and control analysis.[28]

NUMERICAL SIMULATIONS

The procedures outlined in the previous sections of this report have been incorporated into a computer program NCSC - DYNTOCABS (Naval Coastal Systems Center - **DYN**amics of **TO**wed **CAB**le Systems). The following paragraphs outline a set of examples that serve to illustrate the capabilities of the program. Examples of nonlinear, linear, and steady-state analyses are presented. The final example compares the results and execution times of DYNTOCABS with the program CABLE3D.[23]

The first example illustrates a steady-state analysis. Figure 7 shows the side views of two identical cables undergoing a steady 5-knot (8.345-ft/sec) forward tow. The cables are 100 feet in length, 1 inch in diameter, and weigh 1 lb/ft. At the end of each cable is a 10-inch diameter sphere weighing 50 pounds. The cables are depicted by the solid line when submerged and by a dashed line when in air. As is evident from the plot, one of the cases represents a fully submerged cable system while the other represents a system towed from 35 feet above the surface. The fully submerged cable remains concave downward over its entire length due to the fluid drag, while the partially submerged system is concave upward in air and concave downward when submerged. Also, since the partially submerged system has less overall fluid drag, its sphere reaches a greater depth relative to the towing vessel.

The second example illustrates a steady-state analysis for a branched system. Figure 8 shows the top and side views of the system undergoing a steady forward tow (solid line) and a steady turn (dashed line). In each case, the ship's forward speed is 1.48 knots (2.5 ft/sec). A steady turn rate of 0.5 radians/sec (28.65 deg/sec) was added to produce a 10-foot diameter steady turn. The cable is approximately 3 feet long from the tow point to the branch point and approximately 3 feet long from that point to the end of the upper branch (in the side view). The lower branch is about 1.8 feet long. The cable has a uniform diameter of 0.163 inches and weighs 0.008979 lb/ft. The upper and lower branches are terminated by a 2-inch diameter sphere weighing 0.246 pounds and

0.492 pounds, respectively. Figure 8 shows that the steady-state configuration of the cable system during the steady turn remains inside the 10-foot diameter circle prescribed by the ship motion and is deeper than the steady-state configuration of the corresponding forward tow.

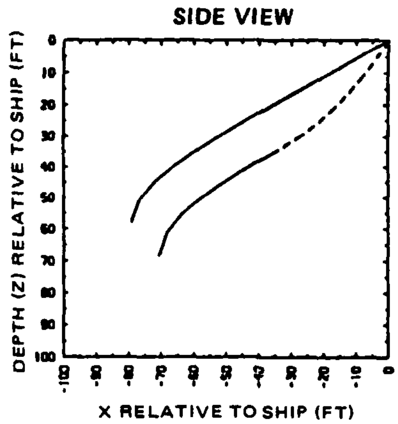

FIGURE 7. SUBMERGED AND PARTIALLY SUBMERGED CABLES DURING A FORWARD TOW

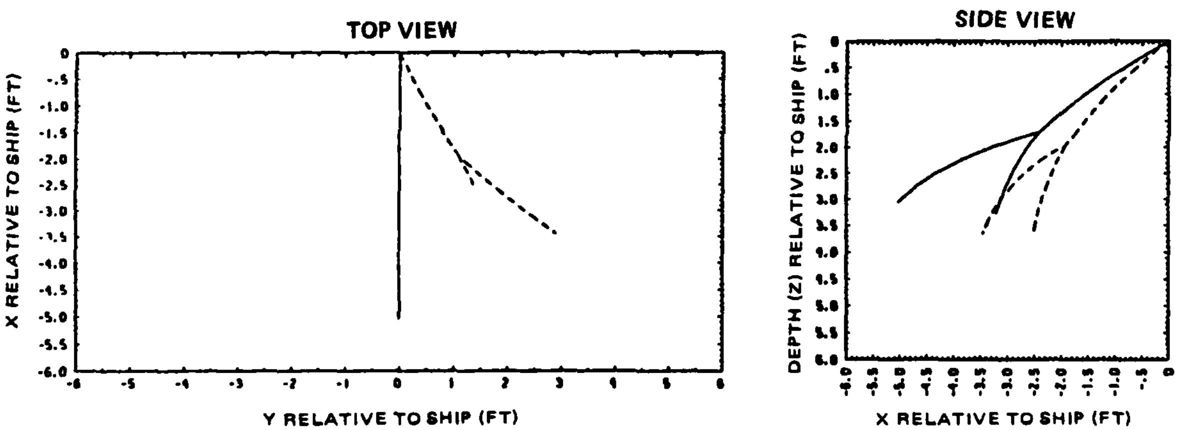

FIGURE 8. BRANCHED CABLE UNDERGOING FORWARD AND CIRCULAR TOW

The next example illustrates the nonlinear time-domain analysis. Figure 9 shows the top and side views of a cable 6 feet in length moving from a steady forward tow of 1.48 knots (2.5 ft/sec) to a steady turn of diameter 10 feet. The cable is 0.163 inches in diameter, weighs 0.008979 lb/ft, and is terminated by a sphere having a diameter of 2 inches and weight of 0.246 pounds. The solid lines represent the respective steady-state configurations and the dashed lines indicate the intermediate positions at 1-second intervals as predicted by the nonlinear time-domain analysis. As time progresses the cable moves inside the circle prescribed by the ship motion and deeper.

The fourth example illustrates the linear and nonlinear time-domain analysis. In this case the cable system of Figure 9 is towed forward at a steady rate of 1.48 knots (2.5 ft/sec). The motion of the tow point is then perturbed by a vertical oscillation. Figure 10 shows the ratio of the vertical displacement of the sphere (relative to its steady-state position) to the excitation amplitude (positive

indicating downward displacements of the sphere) as a function of time for three cases. The dotted line indicates the predictions based on the linearized equations and the solid line indicates the predictions of the full nonlinear equations. The first case has an excitation amplitude of 0.1 feet and frequency of 0.25 cycles per second. Allowing initial transient motions to subside, the sphere begins to oscillate vertically at the forcing frequency and 20 percent of the excitation amplitude. Excellent agreement is found here between the linear and nonlinear equations of motion. In the second case, the excitation amplitude is left unchanged while the frequency is increased to 1 cycle per second. In this case, the predictions based on the linearized equations differ from those based on the nonlinear equations by approximately 10 percent. The sphere no longer oscillates about its original equilibrium position, but oscillates about a point slightly above (negative amplitude ratio) the original position. The linear equations predict oscillations of the same magnitude, but about the wrong position. In the last case, the excitation amplitude is increased to 0.5 feet and the frequency is left unchanged at 1 cycle per second. In this case both the range of the oscillation of the sphere and the location about which it oscillates are inaccurately predicted by the linear equations. For example, the position about which the sphere oscillates is in error by 90 percent.

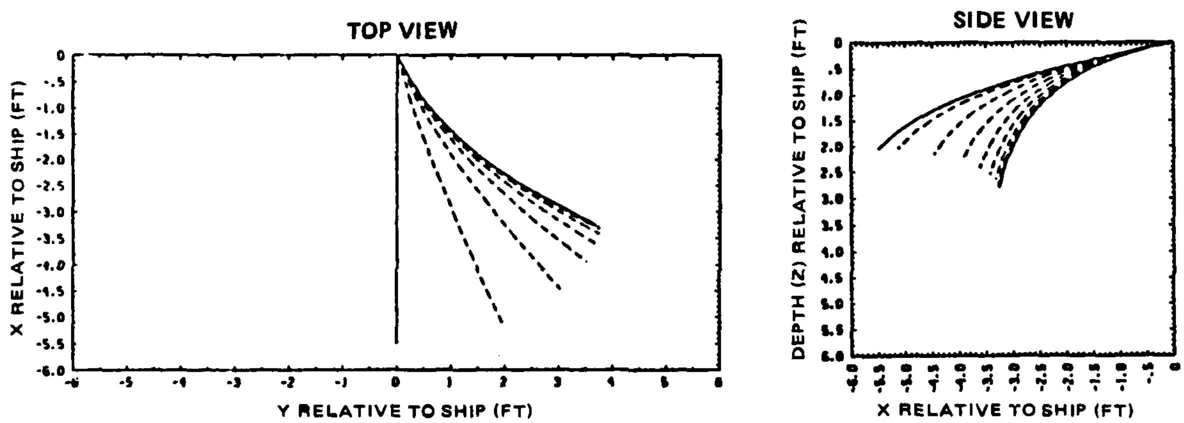

FIGURE 9. CABLE MOTION FROM FORWARD TO CIRCULAR TOW

It should be noted here that much greater nonlinear effects can be induced than those in the previous example. The example simply illustrates how nonlinearities can manifest themselves in towed system response.

The final example compares the results and execution times of DYNTOCABS and CABLE3D[23] and illustrates how both are affected by changes in the number of links used in the model. The modeled segment of cable is 100 feet in length, weighs 0.75 pounds per foot in water, and is assumed to be circular in cross section. It is held fixed at one end and has a 17-pound sphere attached to its free end. The cable is stretched out horizontally and released from rest from that position. Figure 11 shows predictions of the cable shape every 3 seconds from 3 to 30 seconds as calculated by DYNTOCABS and CABLE3D.[23] The results for CABLE3D are shown by dashed lines. Figures 11 (a), (b), and (c) show the results of models having 5, 10, and 15 links. The 5- and 10-link models were generated by breaking the cable into equal length segments, and the 15-link model was generated by halving the lengths of the first two and the last three links of the 10-link model.

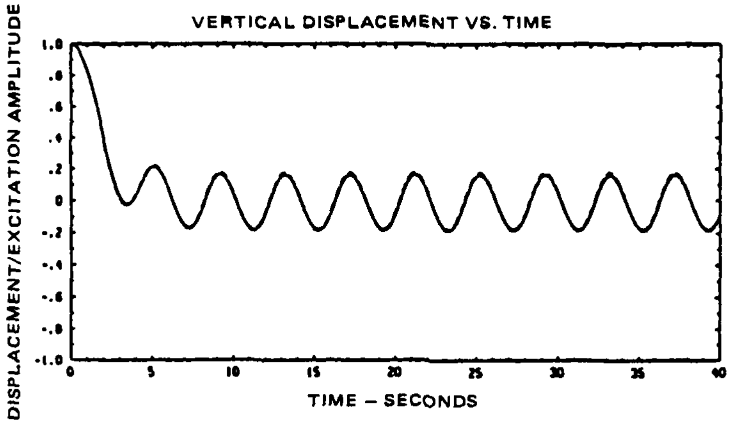

a. Amplitude = 0.1 ft.; Frequency = 0.25 cycle/s

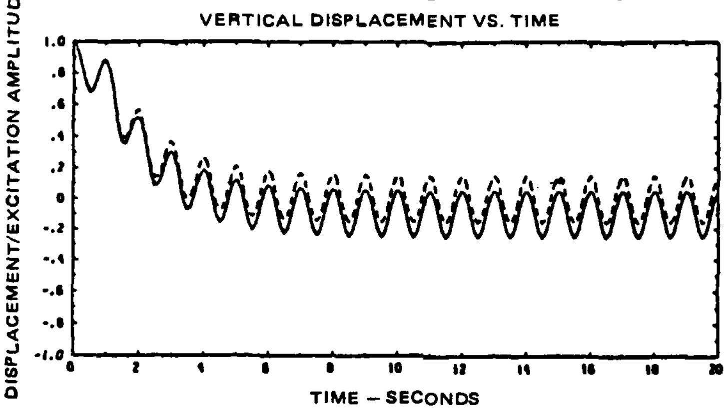

b. Amplitude = 0.1 ft.; Frequency = 1 cycle/s

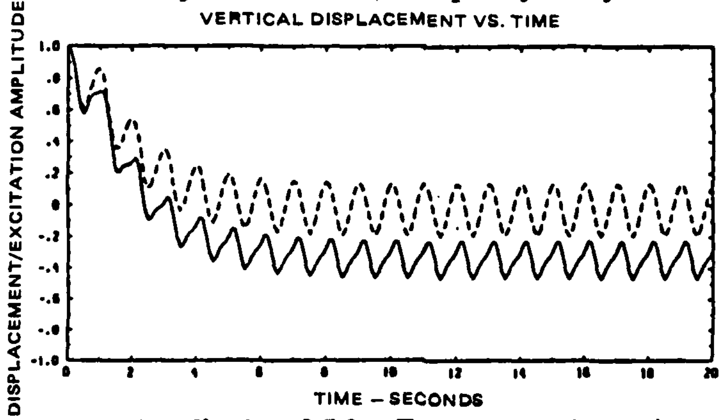

c. Amplitude = 0.5 ft.; Frequency = 1 cycle/s

FIGURE 10. RATIO OF SPHERE DISPLACEMENT TO EXCITATION AMPLITUDE

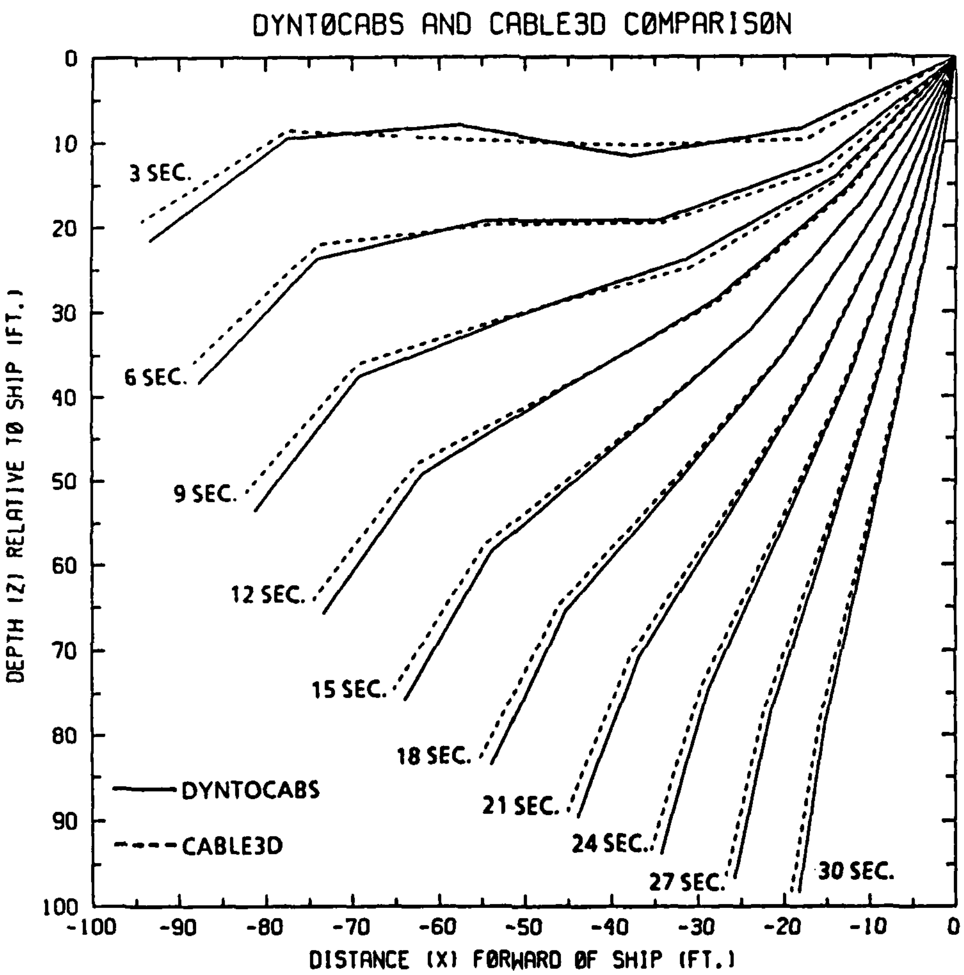

a. 5-Link Model

FIGURE 11. COMPARISON OF DYNTOCABS AND CABLE3D DROP TEST SIMULATIONS FOR A 100-FT CABLE WITH A 17-LB SPHERE ON ITS FREE END (Sheet 1 of 3)

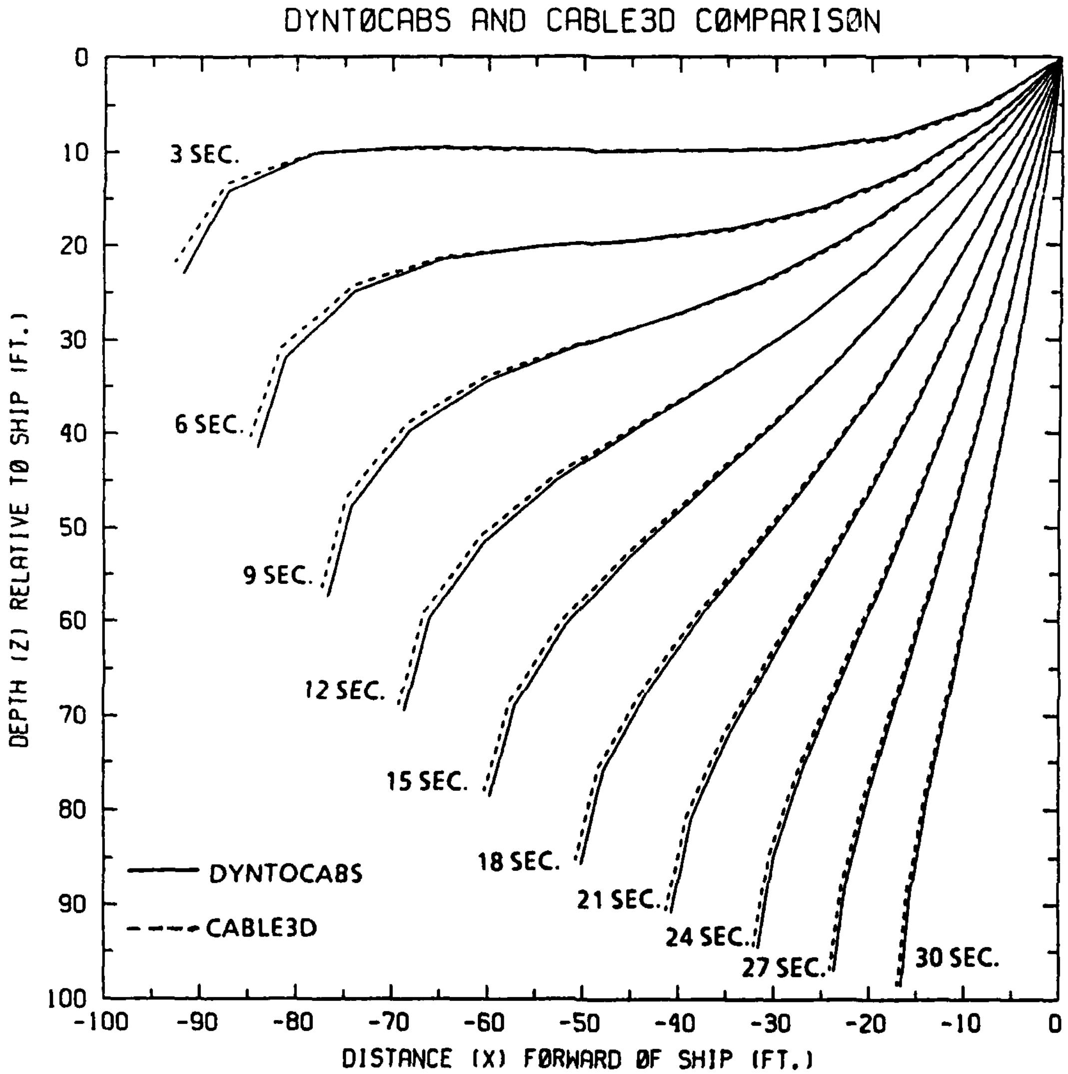

b. 10-Link Model

FIGURE 11. (Sheet 2 of 3)

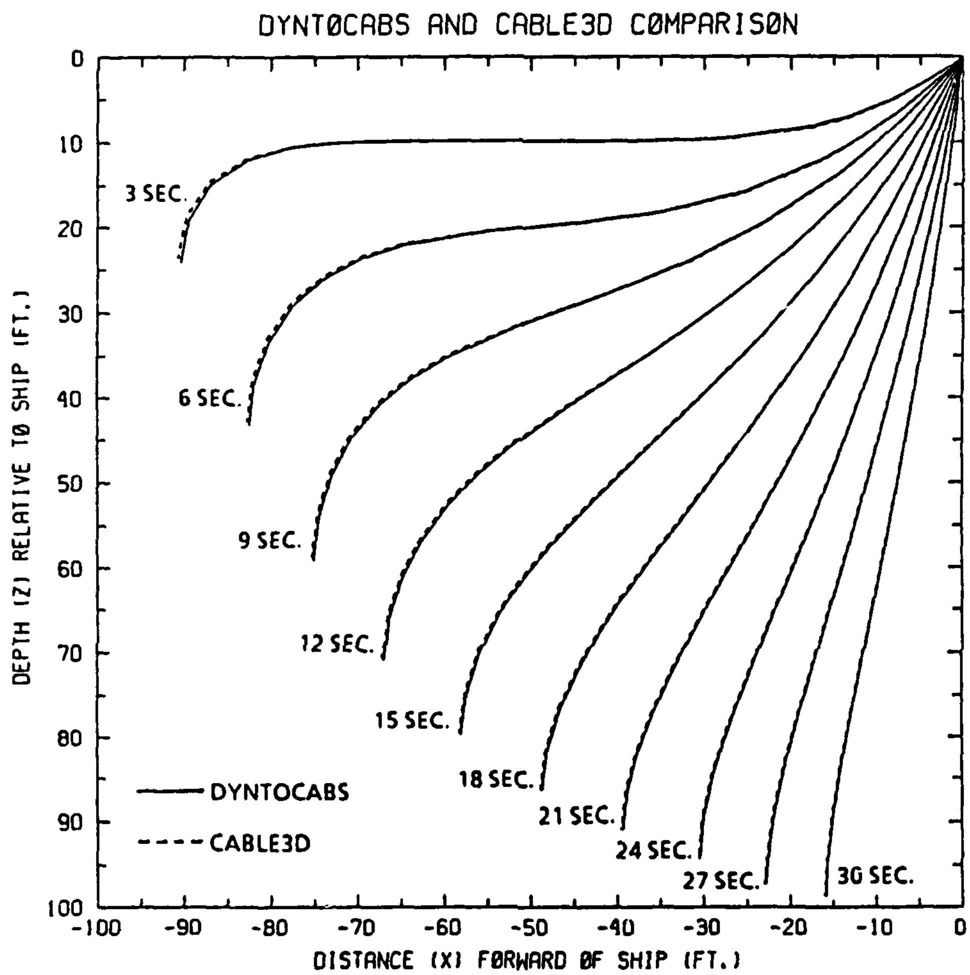

c. 15-Link Model

FIGURE 11. (Sheet 3 of 3)

It is evident from a comparison of Figures 11 (a) through (c) that 5 links is insufficient to model the curvature of the cable as it drops. Although much smoother than the 5-link model, the 10-link model still has difficulty near the fixed and free ends. Moreover, it should be noted that the predictions of the 5- and 10-link models lagged behind those of the 15-link model which appears to adequately describe the system dynamics. In fact, further refined 20- and 30-link models predicted nearly identical results. Finally, although some differences are apparent, the results of DYNTOCABS and CABLE3D agree closely.

Figure 12 shows the execution time in seconds incurred on a VAX 8650 for each of the runs described above (as well as a 20-link model) as a function of the number of links in the model. It is clear that the execution time required by DYNTOCABS is well below that required by CABLE3D, especially as the number of links in the model is increased. DYNTOCABS required one-fifth the execution time that CABLE3D (3D option) required for the 5-link model, and it required one-twenty sixth of the execution time that CABLE3D (3D option) required for the 20-link model.

DISCUSSION

A set of algorithms are presented that have been implemented into a computer code called NCSC - DYNTOCABS. The towed systems may be submerged or partially submerged. They may have one or many open branches, but must be towed from a single point. The physical properties of the cable may change from one segment of the cable to the next. The cable may be attached to a set of towed spheres or more general towed vehicles with control surfaces. The spheres may be located anywhere along the cable, but the towed vehicles must be at the ends of the branches. Finally, the program may be used to perform a linear or nonlinear time-domain or a steady-state analysis. The linear time-domain analysis computes small perturbations to a steady-state configuration due to perturbations in the configuration or perturbations in external inputs, such as the tow point motion and the control surfaces on the towed vehicles. Additional routines may be added to aid in the design of actively controlled towed systems.

The cable is modeled by a series of rigid links connected end-to-end by spherical joints. The masses of these links and the forces that act upon them are lumped at the joints of the system. The effects of fluid drag, buoyancy, weight, and added mass are included. The nonlinear equations of motion of the system are numerically generated using procedures presented herein which are similar to those presented in references 1 and 24. Although exhaustive checks have not been made, the results produced to date using this approach are nearly identical to those found using the approach presented in references 6 and 15. Finally, for the reasons noted in reference 24, substantial increases in execution speed are obtained.

Due to its generality, flexibility, and reasonable execution speed, NCSC - DYNTOCABS is expected to be very useful in the design of large multibranched towed cable systems.

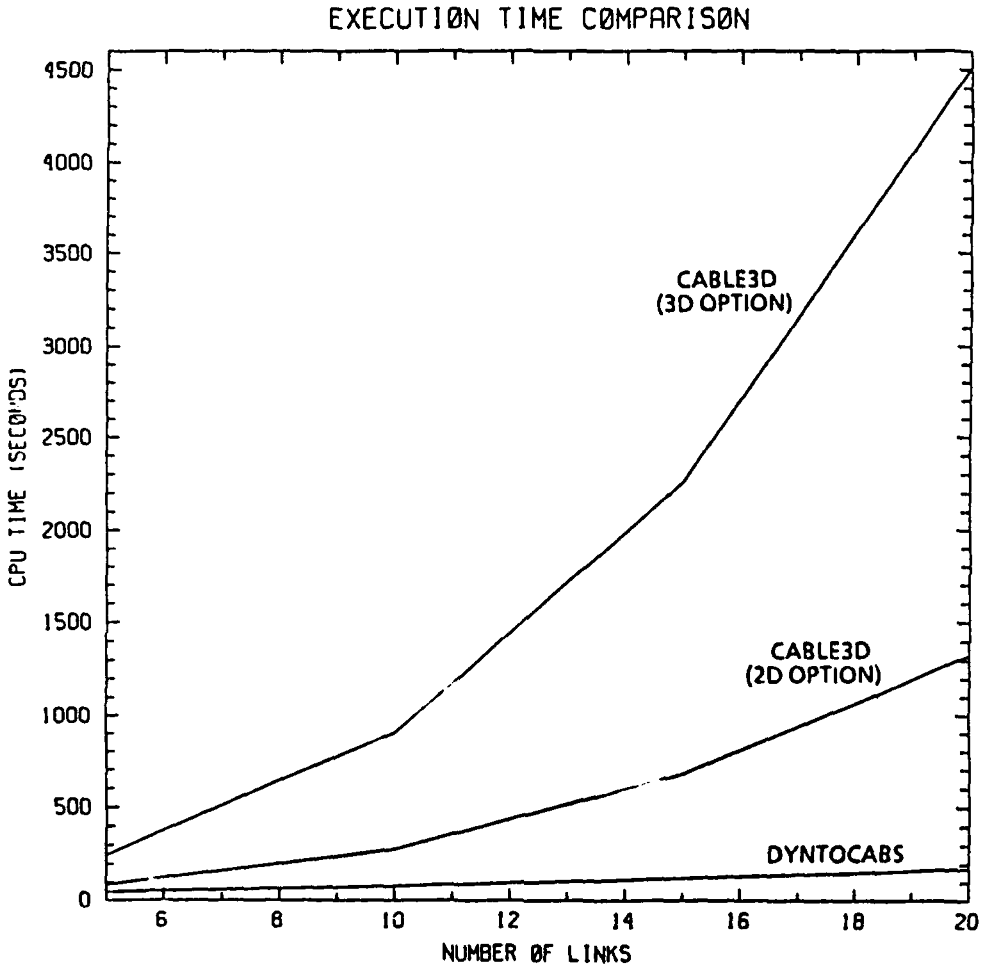

FIGURE 12. EXECUTION TIME COMPARISON BETWEEN DYNTOCABS AND CABLE3D

REFERENCES

1. Walton, T. S., and Polacheck, H., "Calculation of Transient Motion of Submerged Cables," Mathematics of Computation, Vol. 14, pp. 27-46, 1960.

2. Strandhagen, A. G., and Thomas, C. F., "Dynamics of Towed Underwater Vehicles," Report 219, U.S. Navy Mine Defense Laboratory, Panama City, Florida, 1963.

3. Paul, B., and Soler, A. I., "Cable Dynamics and Optimum Towing Strategies for Submersibles," Marine Technical Society Journal, Vol. 6, pp. 34-42, 1972.

4. Leonard, J. W., "Nonlinear Dynamics of Curved Cable Elements," Journal of Engineering Mechanics Division, ASCE, Vol. 99, pp. 616-621, 1973.

5. Webster, R. L., "An Application of the Finite Element Method to the Determination of Nonlinear Static and Dynamic Responses of Underwater Cable Structures," G.E. Technical Information Series Report No. R76EMH2, Syracuse, New York, 1976.

6. Winget, J. M., and Huston, R. L., "Cable Dynamics - A Finite Segment Approach," Computers and Structures, Vol. 6, pp. 475-480, 1976.

7. Leonard, J. W., and Nath, J. H., "Comparison of Finite Element and Lumped Parameter Methods for Oceanic Cables," Engineering Structures, Vol. 3, pp. 153-167, 1981.

8. Sanders, J. V., "A Three-Dimensional Dynamic Analysis of a Towed System," Ocean *Engineering*, Vol. 9, No. 5, pp. 483-499, 1982.

9. Delmer, T. N., Stephens, T. C., and Coe, J. M., "Numerical Simulation of Towed Cables," Ocean Engineering, Vol. 10, No. 6, pp. 443-457, 1983.

11. Milianzzo, F., Wilkie, M., and Latchman, S. A., "An Efficient Algorithm for Simulating the Dynamics of Towed Cable Systems," Ocean Engineering, Vol. 14, No. 6, pp. 513-526, 1987.

12. Choo, Y., and Casarella, M. J., "A Survey of Analytical Methods for Dynamic Simulation of Cable-Body Systems," Journal of Hydronautics, Vol. 7, pp. 137-144, 1973.

13. Huston, R. L., and Kamman, J. W., "A Representation of Fluid Forces in Finite Segment Cable Models," Computers and Structures, Vol. 14, No. 3-4, pp. 281-287, 1981.

14. Huston, R. L., and Kamman, J. W., "Validation of Finite Segment Cable Models," Computers and Structures, Vol. 15, pp 653-660, 1982.

15. Kamman, J. W., and Huston, R. L., "Modeling of Submerged Cable Dynamics," Computers and Structures, Vol. 20, pp. 623-629, 1985.

16. Huston, R. L., Passerello, C. E., and Harlow, M. W., "Dynamics of Multi-Rigid-Body Systems," Journal of Applied Mechanics, Vol. 45, pp. 889-894, 1978.

17. Huston, R. L., and Passerello, C. E., "On Multi-Rigid-Body System Dynamics," Computer and Structures, Vol. 10, pp. 439-446, 1979.

18. Salvadori, M. G., and Schwartz, R. L., *Differential Equations in Engineering Problems*, Prentice-Hall, New York, pp. 401-408, 1954.

19. Woodward, J. H., "Frequencies of a Hanging Chain Support and End Mass," The Journal of the Acoustical Society of America, Vol. 49, No. 5 (Part 2), pp. 1675-1677, 1971.

20. Palo, P. A., "Comparisons Between Small-Scale Cable Dynamics Experimental Results and Simulations Using SEADYN and SNAPLG Computer Models," CEL TM No. M-44-79-5, Civil Engineering Laboratory, Port Hueneme, CA, 1979.

21. Huston, R. L., and Kamman, J. W., "User's Manual for UCIN-CABLE - A Three-Dimensional, Finite-Segment Computer Code for Submerged and Partially Submerged Cable Systems," Report No. ONR-UC-MIE-050-183-15, University of Cincinnati, Cincinnati, OH, 1983.

22. Kamman, J. W., and Huston, R. L., "User's Manual for UCIN-CABLE III - A Two-Dimensional, Finite-Segment Computer Code for Submerged and Partially Submerged Cable Systems," NCSC CR 105-84, Naval Coastal Systems Center, June 1984, UNCLASSIFIED.

23. Guillebeau, C. A., and Ferrer, C. M., "User's Manual for CABLE3D - A Three-Dimensional, Finite-Segment Computer Code for Submerged and Partially Submerged Cable Systems," NCSC TM 464-87, Naval Coastal Systems Center, June 1988, UNCLASSIFIED.

24. Wilson, H., and Wang, L. C., "Computational Methods for 3D Dynamics of Cables," BER Report No. 414-58, Bureau of Engineering Research, University of Alabama, University, AL, 1987.

25. Gertler, M., and Hagen, G. R., "Standard Equations of Motion for Submarine Simulation," NSRDC Report 2510, Naval Ship Research and Development Center, Washington, DC, 1967.

26. Kane, T. R., Likins, P. W., and Levinson, D. A., *Spacecraft Dynamics*, McGraw-Hill, New York, 1983.

27. Brand, L., *Vector and Tensor Analysis*, Wiley, New York, 1947.

28. D'Souza, A. F., and Garg, V. K., *Advanced Dynamics - Modeling and Analysis*, Prentice-Hall, Inc., New Jersey, 1984.

DISTRIBUTION LIST

	Copy No.
Commander, Naval Sea Systems Command, Naval Sea Systems Command Headquarters, Washington, DC 20362-5101	
(Library)	1
Chief of Naval Operations, Navy Department, Washington, DC 20350-2000	2
Commander, David Taylor Research Center, Bethesda, MD 20084-5000	
(Library)	3
(Code 1548)	4
Commanding Officer, Naval Underwater Systems Center, Newport, RI 02840	
(Library)	5
Commanding Officer, Naval Oceans Systems Center, San Diego, CA 92132	
(Library)	6
Director, Naval Oceans Systems Center, Hawaii Laboratory, Kailua, Kaneohe, HI 93863	
(Library)	7
Commanding Officer, Naval Research Laboratory, Washington, DC 20375	
(Library)	8
Commander, Naval Surface Weapons Center, White Oak, Silver Spring, MD 20910	
(Library)	9
Commander, Naval Surface Weapons Center, Dahlgren Laboratory, Dahlgren, VA 22448	
(Library)	10
Superintendent, Naval Academy, Annapolis, MD 21402-5000	
(Library)	11
Superintendent, Naval Postgraduate School, Monterey, CA 93943	
(Library)	12
Chief of Naval Research, 800 North Quincy Street, Arlington, VA 22217-5000	
(Library)	13
Commander, Naval Weapons Center, China Lake, CA 93555-6001	
(Library)	14
Commander, Naval Air Systems Command, Naval Air Systems Command Headquarters, Washington, DC 20361-5101	
(Library)	15

Commanding Officer, Naval Civil Engineering Laboratory, Port Hueneme, CA 93043 (Library)	16
Commanding Officer, Naval Ocean Research and Development Activity, NSTL, MS 39529-5004 (Library)	17
Administrator, Defense Technical Information Center, Cameron Station, Alexandria, VA 22304-6145	18-27